LAWRENCE
LIVERMORE
NATIONAL
LABORATORY

LLNL-JRNL-653204

Expanded Phase Stability of Gd-Based Garnet Transparent Ceramic Scintillators

Z. M. Seeley, N. J. Cherepy, S. A. Payne

April 14, 2014

Journal of Materials Science

Disclaimer

Expanded Phase Stability of Gd-Based Garnet Transparent Ceramic Scintillators

Zachary M. Seeley, Nerine J. Cherepy, Stephen A. Payne

Lawrence Livermore National Laboratory

7000 East Ave.

Livermore CA, 94550

Abstract

Gadolinium-based transparent polycrystalline ceramic garnet scintillators are being developed for gamma spectroscopy detectors. Scintillator light yield and energy resolution depend on many of the ceramic characteristics, including composition, homogeneity, and presence of secondary phases. In order to investigate phase stability dependence on composition, three base compositions: $Gd_3Ga_{2.2}Al_{2.8}O_{12}$, $Gd_{1.5}Y_{1.5}Ga_{2.2}Al_{2.8}O_{12}$, and $Gd_{1.5}Y_{1.5}Ga_{2.5}Al_{2.5}O_{12}$ were studied, and for each composition the rare earth content was varied according to the formula $(Gd,Y,Ce)_3(Y_XGa_{1-X})_2(Ga,Al)_3O_{12}$; where $-0.01 < X < 0.05$. We have found that yttrium and gallium help to stabilize the garnet crystal structure in the ceramics by allowing inter-ionic substitution among the cationic garnet sites. Specifically, a composition of $Gd_{1.49}Y_{1.49}Ce_{0.02}Ga_{2.5}Al_{2.5}O_{12}$ can accommodate approximately 2 at.% excess rare earth ions from the perfect garnet stoichiometry and remain a phase pure transparent ceramic with optimal performance as a radiation detector. This expanded phase stability region helps to enable fabrication of large transparent ceramics from powder with tolerance for flexibility in chemical stoichiometric precision.

Keywords: phase equilibria, polycrystal, and chemical composition

I. INTRODUCTION

Development of scintillators for gamma ray spectroscopy requires simultaneous optimization of a variety of properties. Their effective atomic number should be maximized (in order to effectively interact with ionizing radiation via the photoelectric effect), their light yield under excitation by ionizing radiation (Photons/MeV) should be as high as possible (to minimize the effect of photon statistics), their optical clarity should be excellent (for effective and homogeneous light collection), and their emission spectra should be in the blue-green range (for high efficiency photodetection by standard bialkali photomultiplier tubes). Gd-based garnets offer a unique class of materials capable of high performance in this application.

Transparent ceramics offer advantages in low-cost production and large-size uniformity, compared to single crystals. The great success of YAG (yttrium aluminum garnet) transparent ceramics achieving broad commercial implementation inspired our search for a garnet transparent ceramic scintillator that could supplant single crystal dominance in this field. The simple high-Z analog of YAG, GAG (gadolinium aluminum garnet) is well-known to be difficult to grow due to the limited range of its phase stability, for example, one report of growth of GAG from flux required 25 wt% flux and the small crystals that could be obtained were highly flawed. [1] Generally speaking, single crystals can typically be grown with feedstock that is somewhat off-stoichiometry, since during solidification, excess can be rejected from the as-formed crystals to the top of the boule, for certain melt-growth methods (such as Bridgman) or left behind in the crucible for others (such as Czochralski). In contrast, transparent ceramics require strict adherence to a stoichiometry that can provide the correct crystal phase for the entire volume. Any off-stoichiometric excess will lead to secondary phases and give rise to optically scattering secondary phase inclusions at grain boundaries. For example, the stoichiometry tolerances for YAG powders used

in transparent ceramics fabrication are tight, as it is a line compound. Non-stoichiometric GGAG(Ce) phosphors described in ref. 2 provided insight into the potential flexibility and relationship between the phase stability of Gd garnets and cationic substitution populations. In this paper, we describe our ongoing efforts to engineer a Gd-based garnet, amenable to transparent ceramics processing, via utilization of the principle of inter-substitutional ions to enhance a broad stoichiometric range over which the garnet phase is stable.

After our results published in 2010, demonstrating energy resolution for GYGAG(Ce) of R (662 keV) < 5%,[3] a breakthrough performance for oxide scintillators, many efforts have been made to explore compositions of Gd-based garnets containing inter-substitutional ions.[4-6] Most reports involve single crystal growth, powder synthesis and/or computational techniques, and are aimed at identifying high light yield compositions. One important optimization involves the Ga content: higher Ga provides desirable shorter wavelength emission, but when Ga concentration is too high, the conduction band level is reduced too much, leading to quenching of the Ce^{3+} luminescence.[6]

For a transparent ceramic garnet scintillator for gamma spectroscopy to be commercialized, process conditions must be developed to produce large, homogeneous ceramics, as described in our previous work,[7] and a robust composition that is insensitive to minor process modifications is needed, as addressed in this paper. Here we report on Gd-garnet compositions that are both high light yield, providing excellent gamma ray spectroscopy, and highly phase stable over a broad stoichiometric range, for economical ceramics fabrication. With such compositions, we obtain scintillation providing energy resolution of as good as 4.3% at 662 keV, with PMT readout, and large-size ceramics (>2 in^3) with high optical transparency.[8] These scintillators may be integrated into gamma spectrometers utilizing PMT or silicon photodiode readout to provide spectroscopy superior to that of the standard scintillators, thallium-doped sodium and cesium iodide.[9,10]

II. METHODS

A. Transparent Ceramics fabrication

In order to study the effect of chemical composition on the phase purity of Gd-based garnet ceramics, nanoparticles of the general formula $(Gd,Y,Ce)_3(Ga,Al)_5O_{12}$ were synthesized via the flame spray pyrolysis (FSP) method by Nanocerox Inc (Ann Arbor, MI). Three distinct garnet compositions were studied: GGAG(Ce) ($Gd_{2.98}Ce_{0.02}Ga_{2.2}Al_{2.8}O_{12}$), GYGAG(Ce) ($Gd_{1.49}Y_{1.49}Ce_{0.02}Ga_{2.2}Al_{2.8}O_{12}$), and $GYG_{2.5}AG(Ce)$ with a higher gallium content ($Gd_{1.5}Y_{1.5}Ga_{2.5}Al_{2.5}O_{12}$). In addition, in order to study the allowable concentration of inter-substitutional ions, within each of these three garnets the composition of excess rare earth was varied according to the formula $(Gd,Y,Ce)_3(Y_XGa_{1-X})_2(Ga,Al)_3O_{12}$; where $-0.01 < X < 0.05$.

Nanoparticles were suspended in an aqueous solution containing polyethylene glycol (PEG) and ammonium polymethacrylate (Darvan C-N) using an ultrasonic probe and a high shear Thinky mixer. This suspension was spray dried in a Buchi glass chamber, and the resulting powder was uniaxially pressed at 5 ksi followed by a cold isoatatic press (CIP) at 30 ksi to form the ~50% dense green body. Organics were removed by a heat treatment at 900°C in air. Calcined compacts were then loaded into a Thermal Technologies tungsten element vacuum furnace and sintered under a vacuum of <2×10-6 Torr at 1600°C for 2 h to reach closed porosity and densities of approximately 97%. The sintered samples were then hot isostatically pressed (HIP'ed) under 200 MPa of inert argon gas pressure at 1650°C for 4 h in an American Isostatic Presses tungsten element HIP. Since the samples were closed porosity after vacuum sintering, no canning was necessary during the HIP step. Ceramic surfaces were ground, given an

inspection polish, and wipe-cleaned with acetone and methanol. Defects in the ceramics were imaged on a Zeiss AxioLab.A1 optical Microscope focused into the bulk of the ceramic material.

B. X-ray Diffraction

A Bruker D8 Advance x-ray diffractometer (XRD) equipped with a Cu anode tube operated at 40 kV and 40 mA was used to characterize the polished surfaces of the ceramics. Peak angle for the two most intense peaks was calculated from the center of the full width at half max (FWHM) and used to calculate lattice parameter.

C. Beta-Excited Radioluminescence

Radioluminescence spectra were acquired using a $^{90}Sr/^{90}Y$ source (~1 MeV average beta energy). Spectra were collected with a Princeton Instruments/Acton Spec 10 spectrograph coupled to a thermoelectrically cooled silicon CCD camera.

D. Scintillation Characterization with PMT Readout

Pulse height spectra were measured with a ^{137}Cs source. Samples were optically coupled to a Hamamatsu R6231-100 PMT, which was connected to an Ortec 113 preamplifier, and the signals were shaped with a Tennelec TC 244 spectroscopy amplifier (shaping time of 4 μs) and then recorded with an Amptek MCA8000-A multi-channel analyzer. Spectra were analyzed off-line by non-linear least squares fitting to a Gaussian in order to estimate the energy resolution. Light yields were measured by comparison to a standard YAG(Ce) ceramic from Baikowski.

III. RESULTS AND DISCUSSION

A photograph to display the transparency of the polished ceramics fabricated from various powder compositions is shown in Figure 1. The three different garnet compositions, GGAG(Ce) ($Gd_{2.98}Ce_{0.02}Ga_{2.2}Al_{2.8}O_{12}$), GYGAG(Ce) ($Gd_{1.49}Y_{1.49}Ce_{0.02}Ga_{2.2}Al_{2.8}O_{12}$), and $GYG_{2.5}AG(Ce)$ ($Gd_{1.5}Y_{1.5}Ga_{2.5}Al_{2.5}O_{12}$) are separated by rows, and along each row, the rare earth content is varied according to the formula $(Gd,Y,Ce)_3(Y_XGa_{1-X})_2(Ga,Al)_3O_{12}$, where $-0.01 < X < 0.05$. Samples are lettered for specific reference below. Within each row, the left most samples (A, G, and N) have the smallest composition of rare earths and are actually made from powder that is off of the perfect garnet stoichiometry. These samples all display some amount of degraded transparency, which is likely due to the deficiency in rare earth ions causing precipitation of a gallium or aluminum-rich secondary phase. Transparency of the samples improves as the rare earth content is increased (moving to the right along each row), but transparency eventually degrades again at the far right of each row (samples E, L, and V), this time due to a rare earth-rich secondary phase precipitating at grain. Gallium-containing garnets are well-known to have a range of compositional phase stability due to the ability of Ga and rare earth ions to substitute each other on different sites, i.e. they are not line compounds in the phase diagram.[11,12] However, the most notable result in this work is that the width of this phase stability region is significantly dependent on the composition of the garnet. In the GGAG(Ce) (top row), this region is limited to only three samples (B,C, and D) which span a stability region of $X = 0$ to $X = 0.01$. When we add yttrium to the garnet to make GYGAG(Ce) (middle row), the stability region widens to four samples. And finally, when we increase the gallium content from $Ga_{2.2}$ to $Ga_{2.5}$ to make $GYG_{2.5}AG(Ce)$ (bottom row), this stability region grows to seven samples (samples O through U) corresponding to accommodation of 2% excess rare earth ions.

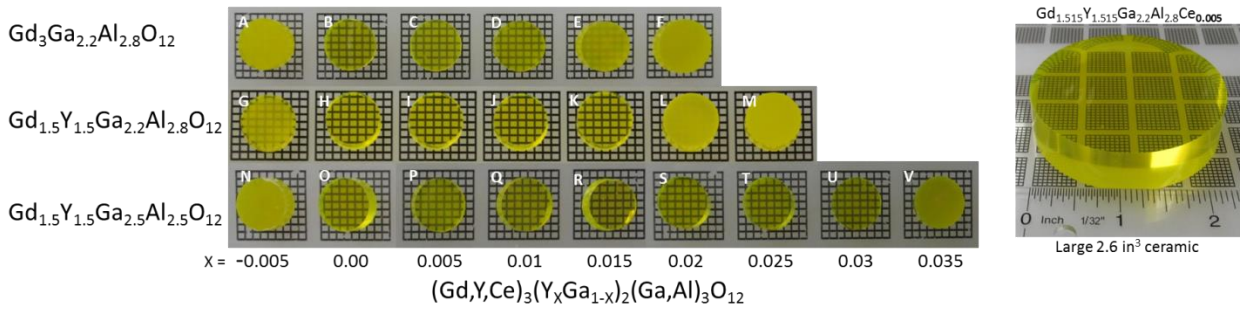

Figure 1. Photographs of Gd-garnet ceramic samples (3 mm thick) made from powder containing different concentrations of excess rare earths and relative amounts of Ga and Al. Individual samples have been labeled with letters for identification throughout the paper. Right photo is of a 2.6 in^3 transparent ceramic GYGAG(Ce).

We attribute the varying ranges of phase stability in these materials to the effect of inter-substitutional ions, i.e. the ability for multiple ions to occupy the same lattice sites. The general formula of the garnets structure has three distinct cationic sites: A, B, and C in the formula $A_3B_2C_3O_{12}$, where A is the 8-fold coordinated dodecahedral site, B is the 6-fold coordinated octahedral site, and C is the 4-fold coordinated tetrahedral site. Due to the different sizes of these sites, there are some size limitations for which metal ions can effectively occupy which sites and form a stable compound. In these compositions, we assume the large dodecahedral site can only be occupied by the large gadolinium, cerium or yttrium ions. The octahedral site can most efficiently be occupied by the intermediate-sized yttrium or gallium ions, and small tetrahedral site can be occupied by the small gallium or aluminum ions. Table 1 lists the ionic radii of the different cations in the garnet structure substitutional sites.

Table 1. Ionic radii of the cations comprising the gadolinium garnets studied in this work.[13]

Cation	8-fold ionic radius (pm)	6-fold ionic radius (pm)	4-fold ionic radius (pm)
Gd	105		
Ce	114		
Y	102	90	
Ga		62	47
Al		53	39

Following this assumption can explain why we see a difference in the size of the phase stability regions in the different garnets in Figure 1. In the GGAG(Ce) top row, we do not have yttrium in the garnet and this forces the dodecahedral site to be occupied solely by gadolinium, which due to its size, is unlikely to occupy any octahedral sites. It is only the gallium and aluminum ions which can participate interionic substitution between octahedral and tetrahedral sites. Limiting the interionic substitution allows the secondary phases to precipitate easier on either end of the compositional spectrum. By adding the yttrium to the garnet in GYGAG(Ce), we have included the possibility for inter-ionic substitution on now all three of the garnet cationic sites. This ionic inter-substitution can allow for a larger deviation from the perfect garnet stoichiometry before secondary phases start to precipitate, thus increasing the phase stability range.

The somewhat unanticipated result from Figure 1 is that with a minimal increase in the gallium content to $GYG_{2.5}AG(Ce)$ (bottom row), the phase stability region grows significantly. This composition should still allow inter-substitutional ions on all three cationic sites, but it appears that this phase stabilization effect is much more efficient at this gallium content.

In order to investigate the possible reason for this expanded phase stability region, x-ray diffraction was performed on a set of the transparent ceramics. Three transparent samples within each of the three garnet compositions were analyzed by XRD: the lowest rare earth content to form transparent samples (samples B, H, and O), moderate rare earth content (samples C, J, and R), and the highest rare earth content to form transparent samples (samples D, K, and U). All peaks for all samples analyzed matched to the Gd-based garnet crystal structure and no secondary phases were visible by XRD, consistent with the samples being transparent. However, a close look at the two most intense peaks for each pattern (shown in Figure 2) reveals some composition-dependent peak shifts. In Figure 2, the three garnet compositions have been grouped together for easier interpretation. In the GGAG(Ce) garnet (bottom of Figure 2), only a slight peak shift to lower angles occurs as the rare earth content increases. This result is consistent with our explanation above considering the limited inter-ionic substitution leading to a small phase stability region. The dodecahedral and octahedral sites are fixed size with gadolinium and gallium ions respectively, and only the inter-substitution of gallium for aluminum on the tetrahedral site can cause lattice expansion and a corresponding peak shift.

When yttrium is added in the GYGAG(Ce) (middle patterns of Figure 2), all the peaks shift to higher angles consistent with a smaller lattice parameter compared with GGAG(Ce), due to the smaller size of the yttrium ion replacing the larger gadolinium ion. In addition, within this group of GYGAG(Ce) ceramics, we notice a significant peak shift to lower angles as the rare earth content increases indicating a stretching of the lattice parameter. This can only occur due to larger ions being forced onto sites that were previously occupied by smaller ions. As the rare earth content increases, some of the yttrium ions spill over onto octahedral sites, replacing the smaller gallium ions. As this happens, more of the gallium ions have to spill over into the tetrahedral sites and replace smaller aluminum ions, leading to an overall larger lattice parameter.

When the gallium content is higher, as in $GYG_{2.5}AG(Ce)$ (top patterns of Figure 2), the peak shift with increased rare earth content is even more pronounced, as is consistent with the broader phase stability region of this material. However, another result from these patterns is that with only a modest (6%) increase in gallium content relative to the GYGAG(Ce) garnet material, we measure a significant peak shift to lower angles, indicating we have stretched the lattice parameter. Therefore the increase in the phase stability region for this composition is attributed to the larger lattice parameter allowing for more efficient inter-ionic substitution of larger ions onto smaller sites in which they would normally not fit, i.e. more yttrium can spill into the octahedral site and more gallium can spill into the tetrahedral site. For comparison, the lattice parameter of GAG, is 12.106 Å.[1]

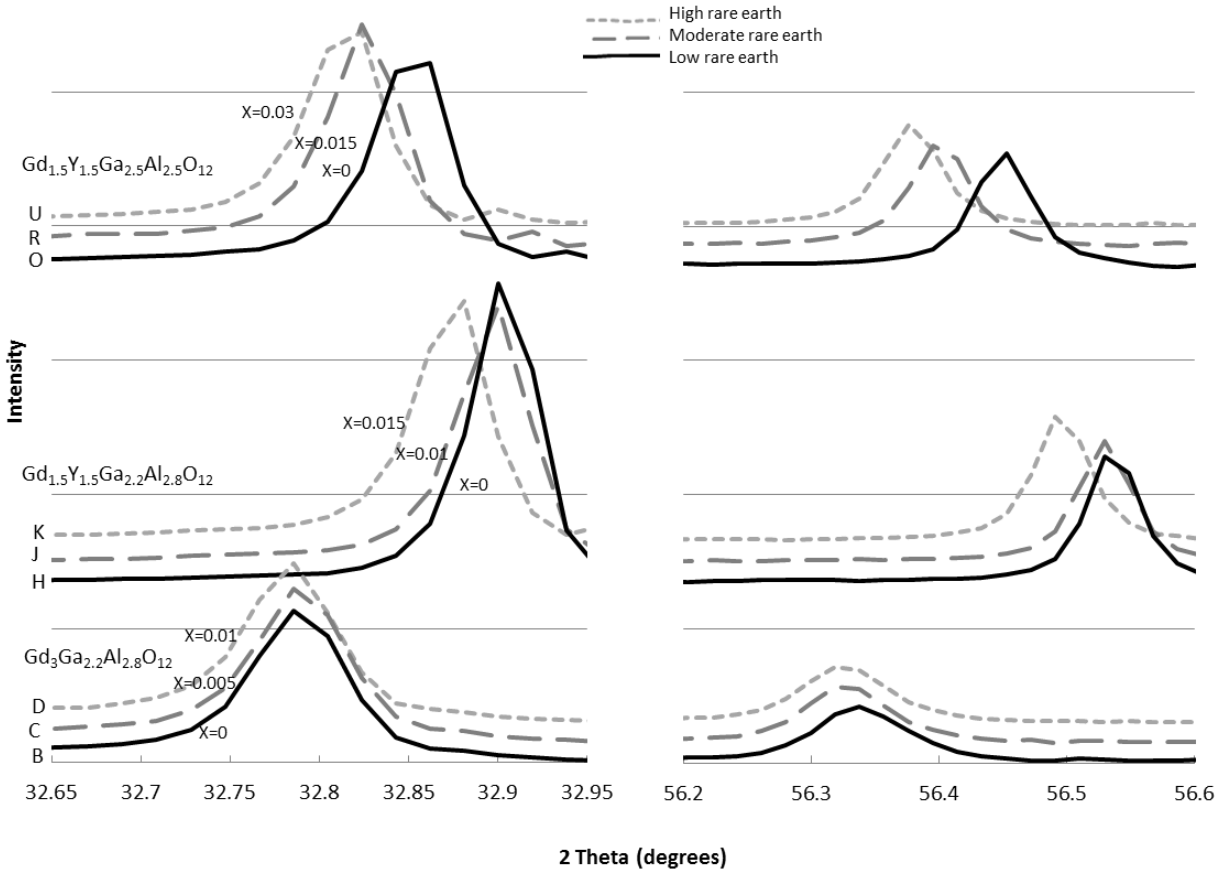

Figure 2. X-ray diffraction patterns for the two most intense peaks in the garnet structure. Patterns are grouped together for the 3 different garnet compositions ($Gd_3Ga_{2.2}Al_{2.8}O_{12}$, $Gd_{1.5}Y_{1.5}Ga_{2.2}Al_{2.8}O_{12}$, and $Gd_{1.5}Y_{1.5}Ga_{2.5}Al_{2.5}O_{12}$), and line type represents rare earth content (Low, Moderate, or High). Patterns have also been labeled by letters according to the sample identities shown in Figure 1.

The x-ray diffraction peak angles and corresponding lattice parameters are summarized in Table 2. In order to put a quantitative description on concentration of inter-ionic substitution we are achieving, X in the formula $(Gd,Y,Ce)_3(Y_XGa_{1-X})_2(Ga,Al)_3O_{12}$ can be calculated from the lattice parameter expansion according to the equation of Brandle and Barns:[12]

$$X = \frac{2\Delta a_\circ}{1.615(r_{RE} - r_m)} \quad (1)$$

where $\Delta a_\circ$ is the stretch in lattice parameter and r_{RE} and r_m are the weighted average for the ionic radii of the rare earth and light metal cations (Ga and Al), respectively. Lattice expansion, with increasing rare earth concentration, is calculated from the peak shift for each of the three garnet materials summarized in Table 1, and a corresponding X is then calculated from equation 1. The concentration of allowable excess rare earth ions calculated from XRD data using equation 1 is in close agreement with the corresponding sample phase stability regions shown in Figure 1. Therefore, we can conclude that the compositions described in Figure 1 are accurate and that excess rare earth ions can be stabilized in the garnet structure. Because the lattice parameter can change and the material stays in the garnet structure, the compositional phase stability is expanded. For the $GYG_{2.5}AG(Ce)$ composition, this corresponds to allowing an excess of 2% rare earth ions into the garnet structure without secondary phase precipitation.

Table 2. X-ray diffraction peak positions and calculated lattice parameters from Figure. 2.

Garnet Composition	Rare earth content (X in Figure 1)	Peak 1 angle	Peak 2 angle	Average Lattice Parameter (Å)	Lattice stretch ($\Delta a_\circ$) Eq.1	X from (Eq. 1)
$Gd_3Ga_{2.2}Al_{2.8}O_{12}$	0	32.787	56.338	12.2085	0.0015	0.0037
	0.005	32.787	56.327	12.2095		
	0.01	32.783	56.326	12.21		
$Gd_{1.5}Y_{1.5}Ga_{2.2}Al_{2.8}O_{12}$	0	32.9	56.436	12.1685	0.009	0.0269
	0.01	32.896	56.530	12.17		
	0.015	32.872	56.496	12.1775		
$Gd_{1.5}Y_{1.5}Ga_{2.5}Al_{2.5}O_{12}$	0	32.849	56.450	12.186	0.014	0.0361
	0.015	32.823	56.400	12.1955		
	0.03	32.812	56.377	12.2		

In addition to the study of lattice parameter, radioluminescence spectra provide information on the Ce^{3+} electronic states in the garnet host. The bluer the emission, the better performance can be obtained with the standard PMTs used for scintillation counting. Figure 3 shows that the beta-excited radioluminescence for the Ga = 2.5 composition of $GYG_{2.5}AG(Ce)$ offers the bluest emission of the three compositions described in this paper.

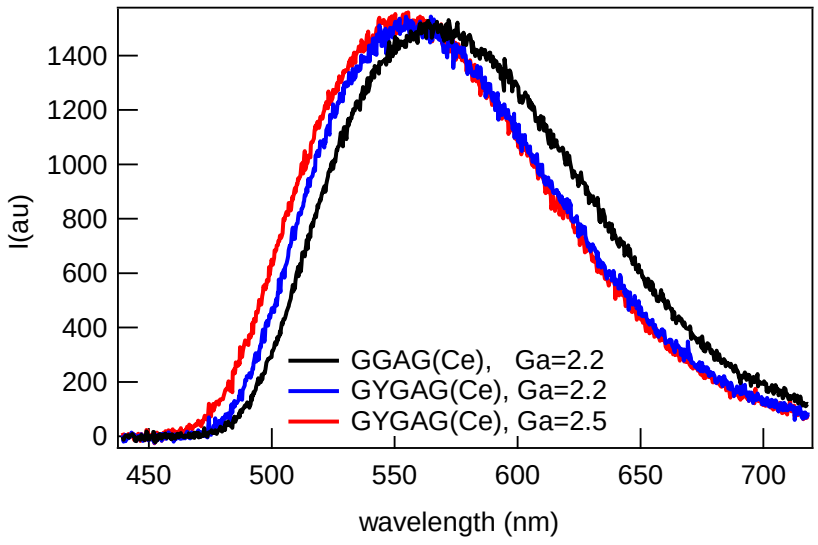

Figure 3. Radioluminescence spectra of GYGAG(Ce) garnets as a function of Ga/Al ratio indicate that emission is blue-shifted with additional Ga. In addition, GGAG(Ce), without Y exhibits a red-shifted emission, compared to the GYGAG(Ce) analog.

For the samples described in in Figures 1 and 3, scintillation performance, including light yield and energy resolution under gamma ray excitation, was obtained and is shown in Table 3. We are developing prototype detectors incorporating GYGAG scintillators, based on both PMT and silicon photodiode readout, since even better energy resolution of R(662 keV) < 3.5% can be obtained with silicon photodetectors.[8] Initial results obtained with the $Gd_{1.48}Ce_{0.02}Y_{1.5}Ga_{2.5}Al_{2.5}O_{12}$ may be improved upon once we optimize the fabrication for this composition.

Table 3. Scintillation performance of Gd-garnet transparent ceramics described in this paper.

Composition	Emission Peak (nm)	Gamma Light Yield w/ PMT (relative)	Energy resolution w/PMT at 662 keV
$Gd_{2.98}Ce_{0.02}Ga_{2.2}Al_{2.8}O_{12}$	570	1.7	5.0%
$Gd_{1.49}Ce_{0.02}Y_{1.49}Ga_{2.2}Al_{2.8}O_{12}$	560	1.8	4.3% (1 cm^3 size) 4.6% (2 in^3 ceramic)
$Gd_{1.49}Ce_{0.02}Y_{1.49}Ga_{2.5}Al_{2.5}O_{12}$	550	2.0	4.6% (initial 1 cm^3 ceramics)
YAG(Ce) from Baikowski	550	1.0	6.7%

IV. CONCLUSION

Cerium doped gadolinium-based garnet transparent ceramics covering a wide compositional range have been fabricated and characterized for their phase stable region. Three base compositions: $Gd_3Ga_{2.2}Al_{2.8}O_{12}$, $Gd_{1.5}Y_{1.5}Ga_{2.2}Al_{2.8}O_{12}$, and $Gd_{1.5}Y_{1.5}Ga_{2.5}Al_{2.5}O_{12}$ were studied and for each composition the rare earth content was varied according to the formula $(Gd,Y,Ce)_3(Y_XGa_{1-X})_2(Ga,Al)_3O_{12}$; where $-0.01 < X < 0.05$. Visual transparency of the polished ceramics indicated that both yttrium and gallium are necessary to expand the phase stability region. XRD-determined lattice expansions correlated well with the explanation that the phase stability region is due to inter-ionic substitution of the various sized ions between the three cationic garnet lattice sites. Scintillator performance for gamma ray spectroscopy showed that all three garnets are suitable materials and offer exceptional energy resolution as compared with other oxides in their class, however the large phase stability region of the $Gd_{1.5}Y_{1.5}Ga_{2.5}Al_{2.5}O_{12}$ composition makes it especially attractive due to the reduced need for precise chemical control and therefor reduced cost in fabrication and commercialization.

ACKNOWLEDGMENTS

The authors appreciate help from Todd Stefanik of Nanocerox for powder production, Jim Peterson with powder processing, Thale Smith for optical microscopy, and Patrick Beck for gamma ray spectroscopy. This work has been supported by the US Department of Homeland Security, Domestic Nuclear Detection Office, under competitively awarded IAA HSHQDC-09-x-00208/P00002. This support does not constitute an express or implied endorsement on the part of the Government. This work was performed under the auspices of the U.S. DOE by Lawrence Livermore National Laboratory under Contract DE-AC52-07NA27344. LLNL-JRNL-

REFERENCES

1. T. Manabe and E. Kazumichi, Crystal Growth and Optical Properties of Gadolinium Aluminum Garnet, Mat. Res. Bull., **6**, 1167-1174, (1971).
2. T. Kanai, M. Satoh, and I. Miura, Characteristic of a Nonstoichiometric $Gd_{3+\delta}(Al,Ga)_{5-\delta}O_{12}$:Ce Garnet Scintillator, J. Am. Ceram. Soc., **91**, 456-462, (2008).
3. N.J. Cherepy, J.D. Kuntz, Z.M. Seeley, S.E. Fisher, O.B. Drury, B.W. Sturm, T.A. Hurst, R.D. Sanner, J.J. Roberts, S.A. Payne, Transparent ceramic scintillators for γ spectroscopy and radiography, Proc. SPIE, 7805, 7805-01 (2010).
4. K. Kamada, T. Yanagida, J. Pejchal, M. Nikl, T. Endo, K. Tsutumi, Y. Fujimoto, A. Fukabori and A. Yoshikawa, Scintillator-oriented combinatorial search in Ce-doped $(Y,Gd)_3(Ga,Al)_5O_{12}$ multicomponent garnet compounds, J. Phys. D: Appl. Phys., **44**, 505104 (2011).
5. Dorenbos, P. Electronic structure and optical properties of the lanthanide activated $RE_3(Al_{1-x}Ga_x)_5O_{12}$ (RE=Gd, Y,Lu) garnet compounds, *J. Luminescence*, **134**, 310-318, (2012).
6. J.M. Ogiegło, A. Katelnikovas, A. Zych, T. Jüstel, A. Meijerink, and C.R. Ronda, Luminescence and Luminescence Quenching in $Gd_3(Ga,Al)_5O_{12}$ Scintillators Doped with Ce^{3+}, J. Phys. Chem. A, **117**, 2479−2484 (2013).
7. ZM Seeley, NJ Cherepy, SA Payne, Homogeneity of Gd-Based Garnet Transparent Ceramic Scintillators for Gamma Spectroscopy, J. Crystal Growth, **379**, 79-83 (2013).
8. N.J. Cherepy, Z.M. Seeley, S.A. Payne, P.R. Beck, O.B. Drury, S.P. O'Neal, K. Morales Figueroa, S. Hunter, L. Ahle, P.A. Thelin, T. Stefanik, J. Kindem, Development of Transparent Ceramic Ce-Doped Gadolinium Garnet Gamma Spectrometers, IEEE Trans. Nucl. Sci., **60**, 3, 2330 (2013).
9. N.J. Cherepy, S.A. Payne, B.W. Sturm, S.P O'Neal, Z.M. Seeley, O.B. Drury, L.K. Haselhorst, B.L. Rupert, R.D. Sanner, P.A. Thelin, S.E. Fisher, R. Hawrami, K.S. Shah, A. Burger, J. O. Ramey, L.A. Boatner, Performance of Europium-Doped Strontium Iodide, Transparent Ceramics and Bismuth-loaded Polymer Scintillators, *Proc. SPIE*, 8142, 81420W (2011).
10. J. Kindem, R. Conwell, Z.M. Seeley, N.J. Cherepy, S.A. Payne, Performance Comparison of Small GYGAG(Ce) and CsI(TI) Scintillators with PIN Detectors, IEEE Nuclear Science Symposium, Conf. Record, (2011).
11. J. Nicolas, J. Coutures, and J. P. Coutures, Sm_2O_3-Ga_2O_3 and Gd_2O_3-Ga_2O_3 Phase Diagrams, J. Solid State Chem. **52**, 101-113 (1984).
12. C. D. Brandle and R. L. Barns, Crystal Stoichiometry of Czochralski Grown Rare-Earth Gallium Garnets. J. Crystal Growth **26** 169-170 (1974).
13. R.D. Shannon, Revised Effective Ionic Radii and Systematic Studies of Interatomic Distances in Halides and Chalcogenides, Acta Cryst. **A32** 751-767 (1976).